# Testing the Cenozoic multisite composite $^{18}O$ and $^{13}C$ curves: new monospecific Eocene records from a single locality, Demerara Rise (Ocean Drilling Program Leg 207)

Journal Item

# Testing the Cenozoic multisite composite $\delta^{18}O$ and $\delta^{13}C$ curves: New monospecific Eocene records from a single locality, Demerara Rise (Ocean Drilling Program Leg 207)

Philip F. Sexton,[1] Paul A. Wilson,[1] and Richard D. Norris[2]

Received 2 December 2005; revised 16 February 2006; accepted 9 March 2006; published 16 June 2006.

[1] Until recently, very few high-quality deep ocean sedimentary sections of Eocene age have been available. Consequently, our understanding of Eocene paleoceanography has become heavily reliant on "composite" records patched together from multiple sites in different ocean basins and generated using multiple taxa (potential sources of "local" noise in the global signal). Here we test the reliability of the early to middle Eocene composite $\delta^{18}O$ and $\delta^{13}C$ stratigraphies (Zachos et al., 2001) by generating new monospecific records in benthic foraminiferal calcite from a single locality, Demerara Rise, in the tropical western Atlantic (Ocean Drilling Program Leg 207). We present new stable isotope correction factors for commonly used Eocene benthic foraminiferal species. We find that interspecies isotopic offsets are constant across the isotopic range, supporting the notion that the inconstant intertaxa offsets reported elsewhere result from mixing species within genera. In general, the $\delta^{18}O$ stratigraphy from Demerara Rise supports the validity of the Eocene $\delta^{18}O$ composite, while revealing a temporary warming punctuating middle Eocene cooling. This warming may correspond to the so-called "Middle Eocene Climatic Optimum" previously documented in the Southern Ocean. The composite and Demerara Rise records for $\delta^{13}C$ differ substantially. By removing the intersite and intertaxa sources of uncertainty in $\delta^{13}C$, we obtain a clearer picture of carbon cycling during the Eocene. Secular change in interocean $\delta^{13}C$ gradients through the Eocene reveals that intervals of climatic warmth (especially the early Eocene) are associated with very small water mass ageing gradients.

**Citation:** Sexton, P. F., P. A. Wilson, and R. D. Norris (2006), Testing the Cenozoic multisite composite $\delta^{18}O$ and $\delta^{13}C$ curves: New monospecific Eocene records from a single locality, Demerara Rise (Ocean Drilling Program Leg 207), *Paleoceanography*, *21*, PA2019, doi:10.1029/2005PA001253.

## 1. Introduction

[2] Reconstructions of early Cenozoic marine temperatures based on oxygen isotope paleothermometry in foraminiferal calcite indicate that the Eocene (~34 to 55 Ma) was the last great interval of pronounced global warmth. Temperatures of surface waters at high latitude [e.g., *Stott et al.*, 1990; *Barrera and Huber*, 1991] and of intermediate to deep ocean waters globally (Figure 1) are thought to have been as much as 12°C warmer than today, with terrestrial records suggesting even warmer temperatures for the high-latitude continental interiors (up to ~24°C warmer than today [e.g., *Greenwood and Wing*, 1995]). Such extreme warmth by modern standards is widely attributed to high levels of greenhouse gases, mainly carbon dioxide, in the Eocene atmosphere. Despite considerable uncertainty over the precise levels of carbon dioxide attained, estimates ranging from about 2 to 6 times the preanthropogenic level, the concept of an early Eocene "greenhouse climate" akin to that of the mid-Cretaceous [e.g., *Larson*, 1991; *Barron et al.*, 1995; *Wilson and Norris*, 2001; *Bice and Norris*, 2002; *Wilson et al.*, 2002] is well established [*Berner et al.*, 1983; *Sloan and Rea*, 1996; *Ekart et al.*, 1999; *Pearson and Palmer*, 2000; *Berner and Kothavala*, 2001; *Huber and Sloan*, 2001; *Shellito et al.*, 2003; *Pagani et al.*, 2005]. Yet virtually nothing is known of the magnitude and stability of Eocene warmth and carbon cycling on anything but a long-term (multimillion year) timescale.

[3] To a large extent our poor understanding of Eocene palaeoceanographic and palaeoclimatic stability arises simply from a lack of appropriate deep sea sections on which to work. Globally, deep ocean sedimentary sections through the Eocene are plagued by recovery problems associated with widespread chert deposition, spot coring associated with earlier Deep Sea Drilling Project (DSDP) strategies, condensation horizons, hiatuses spanning multiple biozones and poor preservation of carbonate microfossils. These problems are particularly evident across the lower/middle Eocene boundary which is represented in the deep ocean drill sections essentially by a ~1- to 2-Myr-long global hiatus [*Aubry*, 1995; *Norris et al.*, 2001]. For these reasons, even the most comprehensive of existing deep ocean stable isotope records for the early and early middle Eocene are of extremely low temporal resolution (at best one sample per 250 kyr in any one specific drill site) and of discontinuous

[1] National Oceanography Centre, Southampton, School of Ocean and Earth Science, Southampton, UK.
[2] Geosciences Research Division, Scripps Institution of Oceanography, La Jolla, California, USA.


0883-8305/06/2005PA001253$12.00

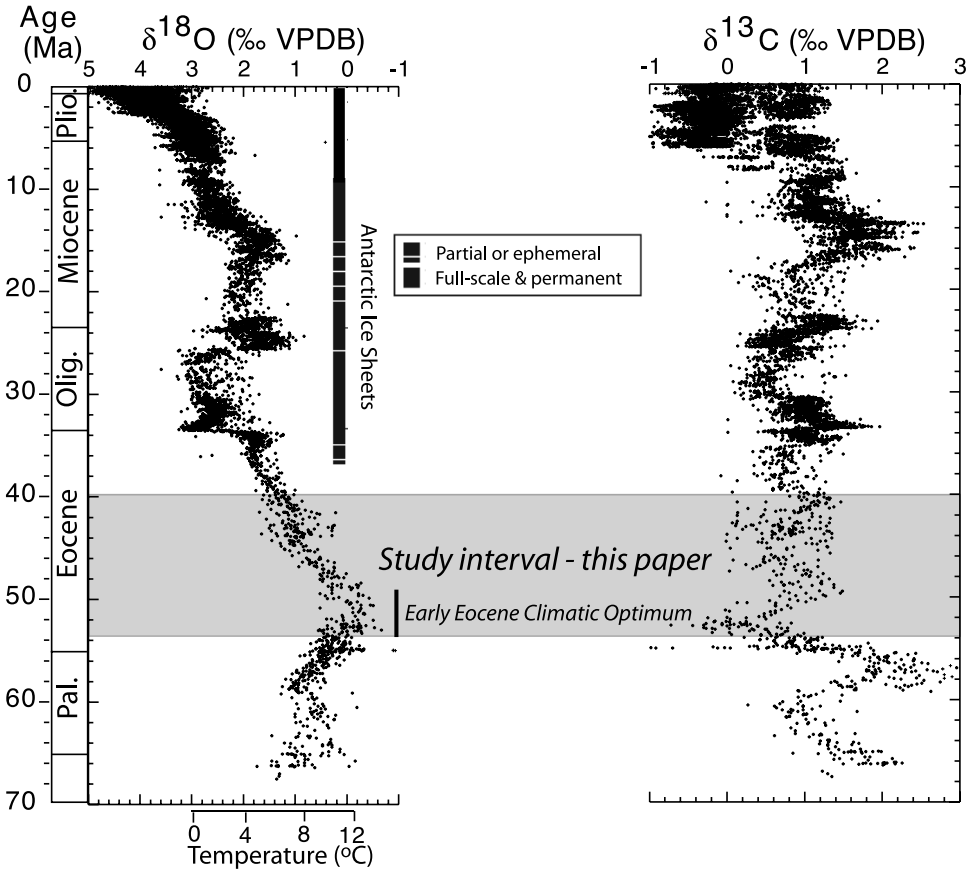


**Figure 1.** Composite deep-sea benthic foraminiferal $\delta^{18}O$ and $\delta^{13}C$ records from many different ocean drilling sites (individual unsmoothed and nonaveraged data points [after *Zachos et al.*, 2001]). Note the paucity and spread of data for pre-Oligocene time. Shaded zone highlights the interval of study in this work. Benthic foraminiferal $\delta^{18}O$ data are corrected for disequilibrium fractionation with respect to seawater $\delta^{18}O$ using the interspecies offsets given by *Katz et al.* [2003]. The $\delta^{18}O$-temperature scale is computed for an "ice-free ocean" (global mean $\delta^{18}O_w = -1.27$‰ Vienna Peedee belemnite (VPDB)) and thus only applies prior to the onset of large-scale glaciation on Antarctica. Vertical bars show qualitative representation of ice volume with respect to Last Glacial Maximum; dashed bars represent minimal ice coverage ($\leq$50%); and solid bars represent close to maximum (>50% present).

stratigraphic coverage. As a result, we have come to rely heavily on the classic multisite data composite of *Zachos et al.* [2001] (Figure 1). However, composites such as this one are, necessarily, patched together from the best available (at publication) records from multiple drill sites (11 different sites for the early and middle Eocene alone, Figure 2a). As such, the record shown in Figure 1 is composed of data from different oceans in different water depths with age control of variable quality and has been generated using multiple benthic foraminiferal taxa, frequently identified to genus level only. These complications mean that we cannot simply assume that the pattern of change indicated faithfully reflects the global signal. What are required are new records at higher resolution from a single locality.

[4] Here we test the paleoceanographic reliability of the multisite, multitaxa composite benthic foraminiferal $\delta^{18}O$ and $\delta^{13}C$ stratigraphies for the Eocene by generating new monospecific records from a single locality, Demerara Rise, in the tropical western Atlantic using material recovered during Ocean Drilling Program (ODP) Leg 207 (Figure 2). Our new records, from ODP Sites 1258 and nearby 1260, span a 14-Myr interval from the early Eocene "greenhouse" through the transitional middle Eocene so-called "doubt house" [*Miller et al.*, 1991] preceding the late Eocene to early Oligocene "icehouse." These data allow us to improve constraints on interspecies offsets in stable isotope fractionation for commonly used benthic foraminiferal taxa. To a first order, the $\delta^{18}O$ stratigraphy from Demerara Rise supports the validity of the composite $\delta^{18}O$ record, at least at the multi-Myr timescale. By removal of intersite and intertaxa $\delta^{13}C$ offsets, the Demerara Rise $\delta^{13}C$ stratigraphy provides a clearer signal of changes in carbon cycling through the early to middle Eocene. At higher resolution, our new records also provide preliminary evidence for

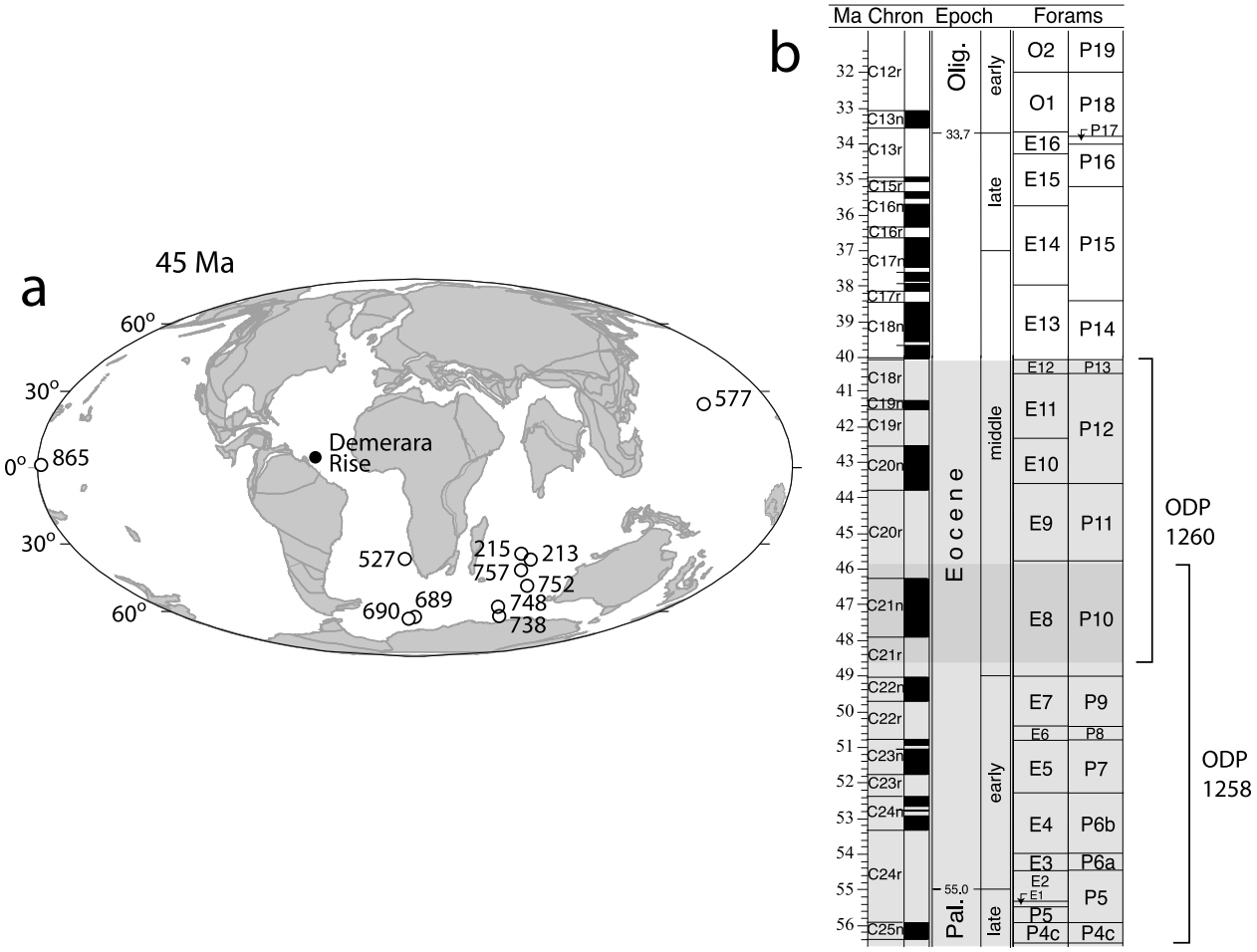


**Figure 2.** (a) Paleogeographic reconstruction for the early middle Eocene (∼45 Ma) showing the location of Demerara Rise (ODP Sites 1258 and 1260) (solid circle) and the 11 different DSDP and ODP Sites that make up the early to middle Eocene portion of the composite record (open circles). Paleolatitudes are from *Zachos et al.* [1994], *Bralower et al.* [1995], and *Suganuma and Ogg* [2006]. Paleogeographic map is from the Ocean Drilling Stratigraphic Network Plate Tectonic Reconstruction Service (http://www.odsn.de/odsn/services/paleomap/paleomap.html). (b) Geomagnetic polarity timescale and planktic foraminiferal biostratigraphic zonation for the Eocene. New biozonation scheme using "E" zones is from *Berggren and Pearson* [2005], while that using "P" zones is from *Berggren et al.* [1995]. Shaded areas are the respective stratigraphic intervals of the Eocene epoch recovered at Sites 1258 and 1260. The recovery at both sites is composed of continuous spliced sedimentary sections from multiple offset holes except for short intervals from ∼45 to 47.5 Ma at Site 1258 and ∼45 to 48 Ma at Site 1260 (where recovery is from a single hole).

several episodes of transient climate instability during the early through middle Eocene.

## 2. Eocene Stratigraphy of Demerara Rise

[5] During ODP Leg 207, expanded and shallowly buried Eocene sedimentary sections were recovered from Demerara Rise (paleolatitude ∼1°S) in the tropical western Atlantic (Figure 2a) with pervasive cyclicity in physical property data and good biostratigraphic and magnetostratigraphic age control [*Erbacher et al.*, 2004; *Suganuma and Ogg*, 2006]. A continuous (to magnetochron and biozone level) Paleocene and Eocene sedimentary section of soft nannofossil chalk with foraminifera from magnetochrons C25r to C18r (∼58 to 40 Ma) was recovered at two closely spaced (∼14 km lateral distance) sites: 1258 and 1260. The section recovered at Site 1258 (present water depth 3192 m) comprises the entire early Eocene through early middle Eocene (C24r through C20r; ∼55 to 45.5 Ma) whereas Site 1260 (present water depth 2549 m) recovered younger sediments spanning an 8-Myr period of the middle Eocene (C21r through C18r; ∼48 to 40 Ma) (Figure 2b). Both sites lie on the rifted continental crust of Demerara Rise. The northern edge of the Demerara plateau is thought to have subsided rapidly

after initial rifting and reached water depths close to the present by late Cenomanian time [*Arthur and Natland*, 1979]. Eocene Demerara Rise benthic foraminiferal assemblages are typically dominated by the following taxa: *N. truempyi*, *C. eoceanus* (*tuxpamensis* morphotype), *C. grimsdalei*, *C. subspiratus*, *Gyroidinoides* spp., *O. umbonatus*, *Stilostomella* sp., *C. havanensis*, *Globocassidulina subglobosa*, and *Karreriella* sp., with *H. cushmani*, *O. mexicana* and *Vulvulina* sp. becoming additional components in the later middle Eocene. Paleodepth interpretations based on this benthic foraminiferal fauna corroborate the interpretation of a paleodepth that was close to modern during the Eocene. Thus data presented here are indicative of upper abyssal (~2500 to 3200 m) water mass properties during the Eocene.

## 3. Methods

### 3.1. Sampling Strategy and Age Model

[6] A complete and well defined paleomagnetic reversal stratigraphy has been developed for the Eocene sections at Sites 1258 and 1260 [*Erbacher et al.*, 2004; *Suganuma and Ogg*, 2006]. An age model for these sections was generated by assuming linear sedimentation rates between the well-constrained (approximately ±60 kyr) paleomagnetic reversals documented for both sites (Figure 3). Numerical ages were applied using the *Cande and Kent* [1995] timescale. Sedimentation rates for early and middle Eocene sedimentary sections at Demerara Rise are, on average, relatively high compared to the majority of deep sea sections of this age. Generally, average linear sedimentation rates for the lower Eocene range between about 1 and 2 cm/kyr but are distinctly higher within C24n (52.4 to 53.3 Ma, ~4 cm/kyr). Sedimentation rates decrease in the lower middle Eocene (C21r to C20r, ~1 cm/kyr), while an increase in sedimentation rates to an average of ~2 cm/kyr occurs during the remainder of the middle Eocene (C20n to C18r). Sections were sampled (sample volume = 20 cc) at approximately 150 cm spacing routinely, with higher-resolution sampling in intervals of particular interest (e.g., ~40.3 Ma and from 42 to 44 Ma). Consequently, the temporal resolution of our records from both Sites 1258 and 1260 typically varies between 30 and 100 kyr (a result of variable sedimentation rates) throughout the early through middle Eocene, but occasionally reaches as high as 10 kyr in several discrete intervals (e.g., ~40.3 Ma and 52.4 to 53.3 Ma [C24n] because of higher sampling density and higher sedimentation rates, respectively).

### 3.2. Benthic Foraminifera

[7] Sediments were disaggregated by soaking in deionized water for 30 min and wet sieving through a 63 μm mesh. The coarse fraction was dry sieved and benthic foraminifera were picked from the 250 to 400 μm size fraction. ODP Sites 1258 and 1260 contain abundant and diverse calcareous benthic foraminifera. Species from the genera *Cibicidoides* and *Nuttallides* were used for monospecific stable isotope analyses because there is much evidence, especially from the Neogene, to suggest that species from these genera possess relatively constant offsets in their fractionation of stable isotopes from that of "equilibrium" calcite [*Shackleton et al.*, 1984; *Shackleton and Hall*, 1997; *Katz et al.*, 2003]. The two species used for the vast majority of the analyses were *Cibicidoides eoceanus* (*tuxpamensis* morphotype) and *Nuttallides truempyi*. Both species range throughout the entire interval of interest but are thought to have contrasting habitat preferences. *Cibicidoides* spp. are thought to maintain an epifaunal habitat while *Nuttallides* spp. are thought to occupy a shallow infaunal niche below the sediment-water interface, based on distributions of live foraminiferal assemblages in modern sediments [*Jorissen et al.*, 1998] and compilations of existing stable isotope data from fossil assemblages [*Shackleton et al.*, 1984; *Katz et al.*, 2003]. *Cibicidoides subspiratus* was also occasionally used for monospecific stable isotope analyses where abundances of *C. eoceanus* temporarily declined. Benthic foraminiferal taxonomy follows that of *Tjalsma and Lohmann* [1983] and *van Morkhoven et al.* [1986].

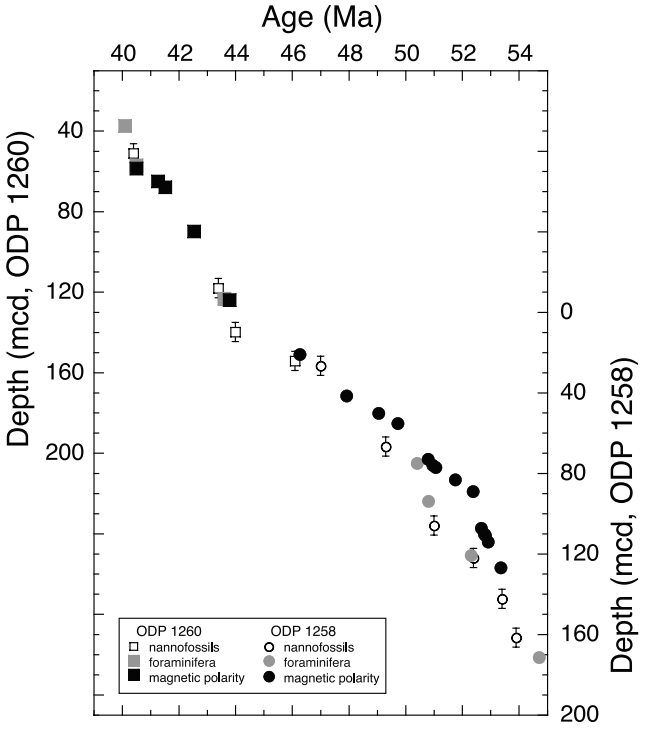


**Figure 3.** Age-depth plot for the early through middle Eocene sedimentary sections at Demerara Rise: ODP Sites 1258 and 1260. Shown are the distribution of age datums for paleomagnetic reversals and foraminiferal and nannofossil first and last appearance datums. The age model for Demerara Rise used in this work was developed using the paleomagnetic reversal datums because (1) the sequence of paleomagnetic zones possesses greater resolution than biostratigraphic biozones through the Eocene and (2) paleomagnetic datums at Demerara Rise are better resolved than foraminiferal or nannofossil datums. Error bars are plotted for all datum types, but those for paleomagnetic reversals and foraminifera are smaller than the size of the symbols.

### 3.3. Analytical Methods

[8] Stable isotopes were analyzed on monospecific samples using a Europa Geo 20-20 mass spectrometer equipped with a "CAPS" automatic carbonate preparation system. Between 3 and 14 specimens were analyzed from the 250 to 400 μm size fraction after ultrasonic cleaning in deionized water. Results are reported relative to the Vienna Peedee Belemnite standard (VPDB). Standard external analytical precision, based on replicate analyses of in-house standards calibrated to NBS-19, is ±0.08‰ for $\delta^{18}O$ and $\delta^{13}C$.

## 4. Demerara Rise Benthic Foraminiferal Taphonomy

[9] The majority of Paleogene sections from which published stable isotope data have been generated are, for the most part, characterized by relatively moderate preservation. This taphonomic state is typified by an abundance of micron-scale secondary calcite, dissolution of primary calcite and broad etching of pores, which is clearly seen in benthic foraminiferal calcite from the "classic" DSDP Site 522 (Figure 4a). Examination of the taphonomy of benthic foraminifera from Demerara Rise using scanning electron microscopic (SEM) methods has revealed relatively well-preserved foraminiferal calcite, characterized by a general absence of secondary diagenetic calcite, a relatively smooth unaltered interpore surface texture and a lack of etching around pores (Figures 4b–4d). Preservation does decline slightly in Site 1258 in the lower Eocene, as indicated by a small degree of etching around the pores of the spiral side (Figure 4c).

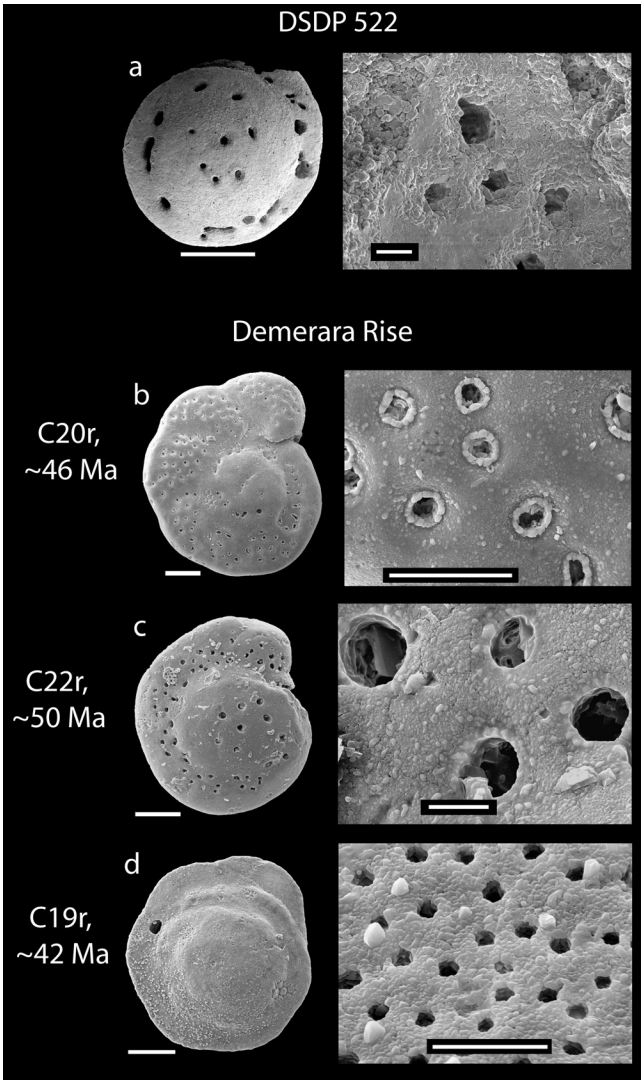


**Figure 4.** Scanning electron micrographs of benthic foraminifera from Demerara Rise and from a "classic" Paleogene drill site (DSDP Site 522). (a) Benthic foraminiferal test (spiral view) and close-up of wall texture of *Cibicidoides havanensis*, DSDP Site 522 (Walvis Ridge). (b) *Cibicidoides eoceanus,* spiral view and close-up view of wall texture on spiral side of same specimen, sample 1258A-2R-5, 47–48.5 cm. Compare Figures 4a and 4b. Note the very good preservation of the specimen in Figure 4b from Site 1258 (Demerara Rise). The significantly poorer preservation (etched pores and abundance of micron-scale secondary calcite) in DSDP Site 522 material (Figure 4a) is typical for the majority of Palaeogene sections from which published stable isotope data have been generated. (c) *C. eoceanus*, spiral view and close-up view of wall texture on spiral side of same specimen, sample 1258A-7R-4, 127–128.5 cm. This individual is from a deeper part of the section (lower Eocene) and exhibits more moderate preservation compared to Figure 4b. (d) *Nuttallides truempyi*, umbilical view and close-up view of wall texture on spiral side of same specimen, Site 1260. Sample 1260A-10R-5, 50–54 cm. This material displays the relatively good preservation which characterizes the middle Eocene at Site 1260. Scale bars in Figures 4a–4d are 100 μm (left side) and 10 μm (right side).

## 5. Eocene Benthic Foraminiferal Interspecies Stable Isotope Offsets

[10] When studying geologically long time periods where the fluctuating faunal composition of the foraminiferal assemblage prevents one single species from being used throughout, calculation of interspecies stable isotope offsets is desirable in order that comparable and consistent records can be generated. The two principal species analyzed in this study are *C. eoceanus* and *N. truempyi*. We use ordinary least squares linear regressions to calculate isotopic offsets between these two species, using *C. eoceanus* as the independent variable (Figure 5). Because the regressions for both the $\delta^{18}O$ and $\delta^{13}C$ data sets yield slopes that equal 1 statistically within the 95% confidence interval, we calculate new intercepts with the slopes forced to 1 (Figure 5). These intercepts show that $\delta^{18}O$ offsets between these two species (*C. eoceanus* and *N. truempyi*) are negligible (+0.05‰, n = 108; Figure 5). This negligible $\delta^{18}O$ offset implies that these two species fractionate oxygen isotopes in an almost identical manner. This result provides confidence in intercomparisons between stable isotope data generated from these two commonly used taxa in Paleogene paleoceanographic studies.

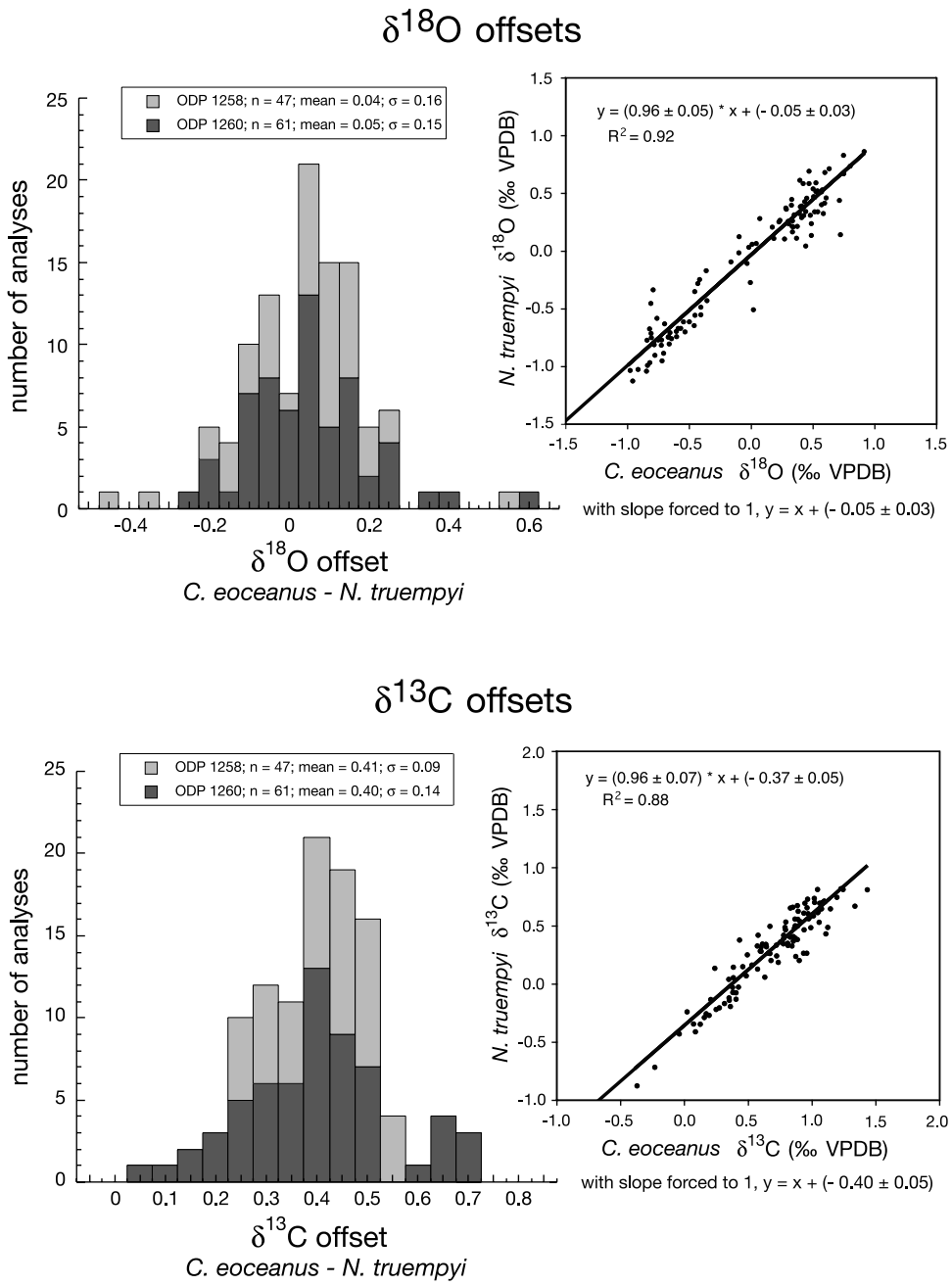


**Figure 5.** Stable isotope offsets between paired analyses of the benthic foraminifera *Cibicidoides eoceanus* and *Nuttallides truempyi* at ODP Sites 1258 and 1260 from Demerara Rise. Interspecies offsets presented here for both $\delta^{18}O$ and $\delta^{13}C$ have slopes that statistically equal 1 at the 95% confidence interval, indicating a constant isotopic offset between individuals in the same size range across the isotopic range (errors for intercepts are also quoted at the 95% confidence interval). This differs from intertaxa $\delta^{18}O$ offsets with a calculated slope <1 [*Katz et al.*, 2003] but supports the notion that there is no a priori reason why interspecies $\delta^{18}O$ offsets between individuals in the same size range should vary according to the absolute $\delta^{18}O$ value of the foraminiferal calcite. The explanation for intertaxa $\delta^{18}O$ offsets with a slope <1 may lie in nondifferentiation of species (which fractionate isotopes to different extents) within a genus (see text).

[11] A constant isotopic offset across the isotopic range (i.e., slope of 1) between paired $\delta^{18}O$ values of two species is expected because there is no obvious a priori reason why interspecies $\delta^{18}O$ offsets between individuals in the same size range should vary according to the absolute $\delta^{18}O$ value of the foraminiferal calcite. However, *Katz et al.* [2003] calculate an offset of "(Nutt. + 0.10)/0.89 = Cib." between *Cibicidoides* spp. and *N. truempyi* $\delta^{18}O$ (Table 1) in their

**Table 1.** Stable Isotope Offsets Between *Cibicidoides* spp. and *Nuttallides* spp. During the Neogene and Paleogene

| | | Adjustment, ‰ | |
|---|---|---|---|
| | Taxa Pairs[a] | $\Delta\delta^{18}O$ | $\Delta\delta^{13}C$ |
| | *Paleogene* | | |
| Demerara Rise (this study) | *Cib. eoceanus*–*Nutt. truempyi* | +0.05 | +0.40 |
| *Katz et al.* [2003] | *Cib.* spp.–*Nutt. truempyi* | +(0.10)/0.89 | +0.34 |
| | *Neogene* | | |
| *Shackleton and Hall* [1997] and *Shackleton et al.* [1984] | *Cib.* spp.–*Nutt.* spp. | +0.50 | 0.00 |

[a]*Cib.*, *Cibicidoides*; *Nutt.*, *Nuttallides*.

analysis of an extensive data set (n = 247) of paired benthic foraminiferal stable isotope data sourced from the literature and from an array of ODP/DSDP Sites through the Paleogene. Although their *y* axis intercept (offset) of +0.10 is in broad agreement with that calculated from Demerara Rise foraminifera (+0.05), the value of the slope (0.89 ± 0.04) calculated by *Katz et al.* [2003] deviates from a slope of 1 which suggests that the $\delta^{18}O$ offsets between *Cibicidoides* spp. and *N. truempyi* are not constant across the isotopic range. Instead, we derive a slope that equals 1 statistically (Figure 5).

[12] Part of the reason for the deviation from a slope of 1 between *Cibicidoides* spp. and *N. truempyi* $\delta^{18}O$ offsets in the *Katz et al.* [2003] Paleogene data set may lie in nondifferentiation of species within the genus *Cibicidoides* [cf. *Katz et al.* [2003]. Stable isotope analyses of multiple species of *Cibicidoides* from Holocene sediments have shown a significant offset between different species [*Curry et al.*, 1993]. The smaller interspecies offset for $\delta^{18}O$ in our work (+0.05‰, versus +0.10‰) may also reflect our use of single, well-defined species of *Cibicidoides* as opposed to a more generic "*Cibicidoides* spp." concept which may be biased by interspecific "vital effects."

[13] Table 1 shows that the mean value for the offset between *Cibicidoides* spp. and *Nuttallides* spp. for both $\delta^{18}O$ and $\delta^{13}C$ during the Neogene differs considerably from that documented in the Paleogene. This temporal difference between genera probably reflects the use of different species within the Neogene and the Paleogene that fractionated stable isotopes to different extents. This observation is attributable to variability in stable isotope fractionation between different species within the same genus, an effect that has been recorded in both core top benthic foraminifera [*Curry et al.*, 1993] and those from Neogene and Paleogene sediments [*Shackleton et al.*, 1984; *Shackleton and Hall*, 1997]. However, it should be borne in mind that the errors for our slopes and intercepts quoted in Figure 5 (and the interspecies offsets in Table 1) do not take into account measurement errors and those related to data reproducibility. Measurement errors are approximately ±0.08‰ for both $\delta^{18}O$ and $\delta^{13}C$ which, when applied to both the independent and dependent variables, yield a combined error in our regressions of ±0.16‰. The error in reproducibility of data in the Demerara Rise sections is typically ±0.04‰ for both $\delta^{18}O$ and $\delta^{13}C$. When combined with the measurement errors, this gives a cumulative additional error (above that quoted in Figure 5) in our regressions of ±0.24‰. In practice, this means that the interspecies stable isotope offsets calculated at Demerara Rise (Table 1; and, by analogy, those from other sedimentary sections) can be considered accurate only to the first decimal place.

[14] Benthic foraminifera from Demerara Rise display interspecies $\delta^{13}C$ offsets that are also broadly consistent with those from the *Katz et al.* [2003] early Paleogene data set (Table 1). The consistently higher $\delta^{13}C$ exhibited by *C. eoceanus* compared to *N. truempyi* (Figure 5) provides support for the paleoecological assumption (based on modern species of *Cibicidoides* and *Nuttallides*) that the former species maintained an epifaunal habitat while the latter species was predominantly shallow infaunal. Epifaunal species, such as the majority of those belonging to the genus *Cibicidoides*, have been used widely to generate paleoceanographic records for the Pleistocene and Pliocene [e.g., *Duplessy et al.*, 1984; *Curry et al.*, 1988; *Sarnthein et al.*, 1988; *de Menocal et al.*, 1992; *Mix et al.*, 1995; *Shackleton and Hall*, 1997], on the grounds that they accurately record true seawater $\delta^{13}C$ [*Belanger et al.*, 1981; *Graham et al.*, 1981; *Shackleton et al.*, 1984; *Shackleton and Hall*, 1997]. Nevertheless, evidence exists to suggest that this epifaunal ecology is associated with an opportunistic life strategy of feeding on the often intermittent flux of labile particulate organic matter ($C_{org}$) to the seafloor [*Rice and Rhoads*, 1989]. Epifaunal species may therefore bloom during periods of high $C_{org}$ flux to the seabed, causing the majority of individuals in deep sea sediments to represent atypical oceanographic conditions [*Jorissen and Wittling*, 1999]. It follows that foraminifera with a shallow infaunal ecology (e.g., *N. truempyi*) may provide a more representative record of mean seawater properties, because of their more sessile ecology. However, despite uncertainties with regards to the precise paleocologies of extinct foraminiferal species, analysis of two or more species with different ecologies (e.g., *C. eoceanus* and *N. truempyi*) has the benefit, at the very least, of providing an independent confirmation of the paleoceanographic trends inferred from the analysis of a single species.

## 6. Foraminiferal Calcite and "Equilibrium" Fractionation

[15] Because $\delta^{18}O$ paleotemperature equations relate $\delta^{18}O$ of foraminiferal calcite to the $\delta^{18}O$ of seawater ($\delta^{18}O_w$), the "vital effect" $\delta^{18}O$ offsets from equilibrium with seawater represent a significant source of uncertainty in $\delta^{18}O$ paleothermometry. One way to tackle this problem is to measure

paired $\delta^{18}O$ on both an extinct species and an extant one. A good example of this strategy is the use of *Oridorsalis umbonatus* to calibrate Paleogene benthic foraminiferal oxygen isotope studies. This species is thought to range from the Coniacian (~86 Ma) to the modern [*Kaiho*, 1998] and its use as a preferred (and underutilized) recorder of ocean conditions during the Paleogene has recently been noted for both Mg/Ca [*Lear et al.*, 2000, 2002] and stable isotope [*Katz et al.*, 2003] data. Measurements on modern core top samples show that, in the modern oceans, *O. umbonatus* secretes its calcite in approximate oxygen isotopic equilibrium with seawater [*Graham et al.*, 1981]. Stable isotope records of fossil tests of *O. umbonatus* suggest that approximate equilibrium $\delta^{18}O$ fractionation in *O. umbonatus* has existed throughout the Cenozoic [*Shackleton et al.*, 1984; *Zachos et al.*, 1992]. If we assume that the extent of isotopic fractionation remains constant throughout a given species' stratigraphic range, then comparison between $\delta^{18}O$ of an extinct species to that of *O. umbonatus* can reveal the extent of isotopic disequilibrium fractionation in the extinct species (note also that variations in environmental parameters such as $[CO_3^{2-}]$ may influence the degree of $\delta^{18}O$ disequilibrium fractionation [*Spero et al.*, 1997]).

[16] Correcting for disequilibrium fractionation is essential to allow accurate calculation of $\delta^{18}O$-derived temperatures. Unfortunately, *O. umbonatus* is not sufficiently abundant at Demerara Rise for stable isotope analysis. Therefore, in order to calculate "equilibrium calcite $\delta^{18}O$" from *Cibicidoides eoceanus* $\delta^{18}O$ values, the *Oridorsalis-Cibicidoides* $\delta^{18}O$ offset of +0.28‰ given by *Katz et al.* [2003] is used. Because the slope of the *Oridorsalis-Nuttallides* $\delta^{18}O$ relationship from *Katz et al.* [2003] is <1 (=0.79), we correct *N. truempyi* for disequilibrium $\delta^{18}O$ fractionation by applying the correction factor for *Nuttallides* of +0.35‰ given by *Shackleton et al.* [1984] and *Shackleton and Hall* [1997].

[17] From the resultant record of equilibrium calcite $\delta^{18}O$, paleotemperatures are calculated using equation (1) of *Bemis et al.* [1998]. This equation was developed for asymbiotic planktic foraminifera, but it is in excellent agreement with a global core top *Cibicidoides* spp. $\delta^{18}O$ calibration for the temperature range from 0° to 7°C. Furthermore, it appears that the modern *Cibicidoides* spp. used in this calibration secrete their tests fairly close to oxygen isotopic equilibrium with seawater, based on the close similarity between equation (1) of *Bemis et al.* [1998] and the inorganic calcite temperature equation of *Kim and O'Neil* [1997].

## 7. Testing the Validity of the Composite Record

[18] The benthic foraminiferal composite $\delta^{18}O$ and $\delta^{13}C$ data shown in Figure 1 are the individual data points from each component drill site. It should be emphasized that, understandably, in order to highlight global Cenozoic trends, *Zachos et al.* [2001] presented their composite record by smoothing these data points (with a five-point running mean) and then fitting a curve using a locally weighted mean. We have chosen to present the individual data points unsmoothed because our purpose is to highlight the intersite and intertaxa variability therein (Figures 6 and 7).

[19] The benthic foraminiferal $\delta^{18}O$ and $\delta^{13}C$ composite data for the early to middle Eocene, plotted according to component drill sites (locations shown in Figure 2a), are shown in Figures 6a and 6b. The $\delta^{13}C$ data from the composite record are also plotted according to foraminiferal genus (Figure 6c). We highlight intertaxa variability only for $\delta^{13}C$ data because Table 1 shows that interspecies offsets in $\delta^{18}O$, calculated using Demerara Rise data, are so small (~0.04‰) compared to the offsets in $\delta^{13}C$ (these are an order of magnitude larger, ~0.40‰). Figures 6a and 6b emphasize the number of different sites (11) that are needed to patch together a composite curve for this 15-Myr-long interval. Because these sites come from different ocean basins and paleowater depths with differing qualities of age control, sources of error are potentially introduced into our understanding of Eocene paleoceanographic evolution. This is particularly apparent for the middle Eocene from 46 to 40 Ma (e.g., the offset between $\delta^{18}O$ data from ODP Sites 690 (Southern Ocean) and 757 (Indian Ocean) around 43 Ma is ~1‰). This degree of divergence in composite $\delta^{18}O$ data prohibits accurate evaluation of global trends in climate change through this interval. For example, Figure 6a shows that the composite $\delta^{18}O$ data from Southern Ocean ODP Sites 689 and 748 indicate an interval of deep ocean warming at about 41.5 Ma: the suggested "Middle Eocene Climatic Optimum" ("MECO") of *Bohaty and Zachos* [2003]. In contrast, the composite data from a mid-Pacific site (ODP 865) and another Southern Ocean site (ODP 690) show no evidence of the proposed MECO around 41.5 Ma (Figure 6a).

[20] The composite $\delta^{13}C$ data display a much greater spread than the composite $\delta^{18}O$ data (Figures 6a and 6b). There are two principal sources of variability in the multisite composite $\delta^{13}C$ record. The first is heterogeneity in seawater $\delta^{13}C$ among drill sites. The second is offsets attributable to the use of different taxa. The extent to which these intersite and intertaxa $\delta^{13}C$ offsets are responsible for the spread in the composite $\delta^{13}C$ data can be gauged by comparing Figures 6b and 6c. Our analysis shows that some of the spread in the composite $\delta^{13}C$ record originates from atypical $\delta^{13}C$ data at particular drill sites, notably ODP Site 865 and ODP Site 757 during the middle Eocene (46 to 40 Ma, Figure 6b), and that some of the spread can be attributed to $\delta^{13}C$ offsets between taxa (Figure 6c). The offsets observed in Figure 6c between "*Cibicidoides* spp." and "*Nuttallides* spp." are in the same direction and of a similar magnitude to those recorded in the Demerara Rise $\delta^{13}C$ data set (Figure 5).

[21] In Figure 7 we compare our new data from Demerara Rise (by species; $\delta^{18}O$ normalized to "equilibrium calcite," $\delta^{13}C$ normalized to *Cibicidoides*, see Figure 5) with the composite data from Figures 6a and 6b. This exercise shows a much better match between the multisite composite and Demerara Rise data sets for $\delta^{18}O$ than for $\delta^{13}C$. First-order $\delta^{18}O$ trends seen in the Demerara Rise records are similar (but not identical) to those seen in the multisite composite (Figure 7a). In both data sets the lowest $\delta^{18}O$ values of the

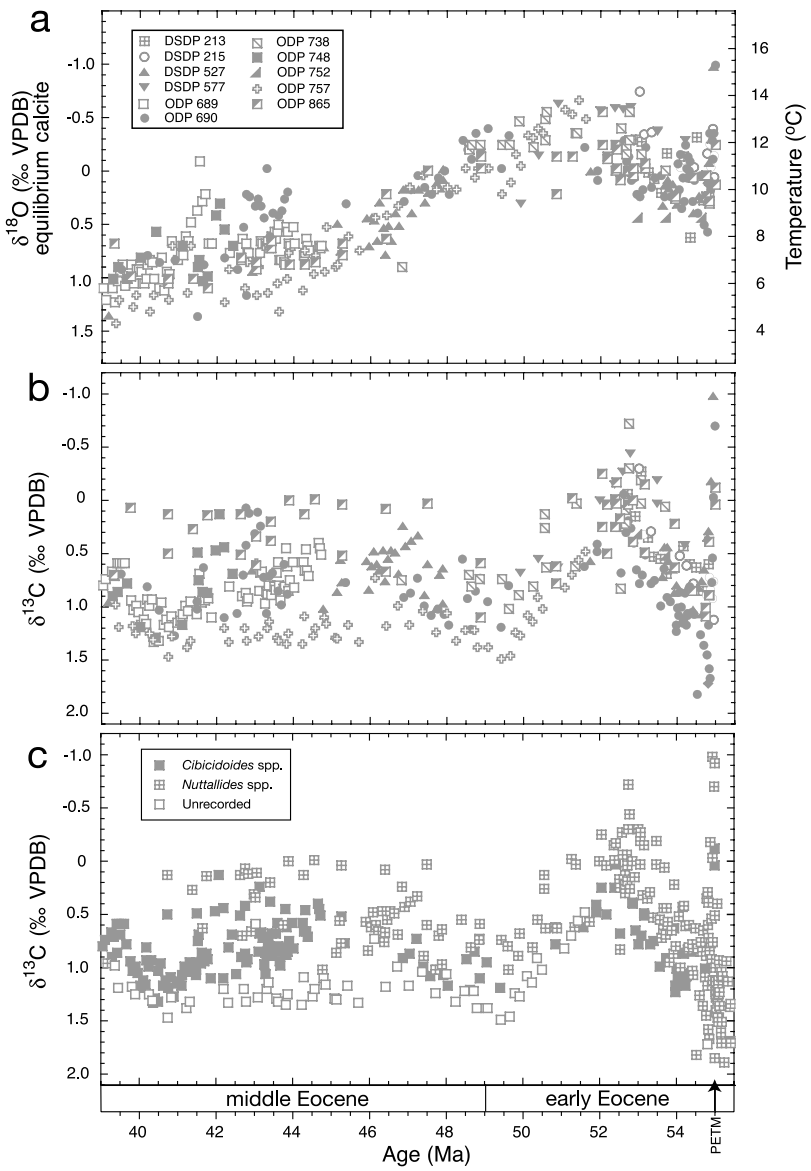


**Figure 6.** Composite multisite deep-sea benthic foraminiferal $\delta^{18}O$ and $\delta^{13}C$ records (individual unsmoothed data points from Figure 1) for the early to middle Eocene. (a) The $\delta^{18}O$ data from component drill sites. (b) The $\delta^{13}C$ data from component drill sites. Data symbols for different drill sites are the same as in Figure 6a. (c) The $\delta^{13}C$ data plotted according to benthic foraminiferal "taxa" (genus). Data shown are individual $\delta^{13}C$ data points from the composite record, displaying clear separation between taxa.

early Eocene occur at about 50.5 Ma and $\delta^{18}O$ values increase across the early/middle Eocene boundary and trend to higher $\delta^{18}O$ to about 44 Ma (Figure 7a). The new data then provide clear support for a temporary reversal (~44 to 42 Ma) in the long-term $\delta^{18}O$ increase after the early Eocene Climatic Optimum, a feature not clearly depicted in the composite data. The $\delta^{18}O$ data then increase from about 42 Ma up to ~40.35 Ma, at which point a large-amplitude (~1.3‰) negative excursion occurs. This excursion is not evident in the lower-resolution composite data. Notably, the data from Demerara Rise show no evidence for deep ocean warming at 41.5 Ma.

[22] By removing both the intersite and intertaxa sources of variability in $\delta^{13}C$, we appear to have obtained a clearer signal of changes in carbon cycling through the middle Eocene (Figure 7b). The new $\delta^{13}C$ data confirm that the most negative $\delta^{13}C$ values seen in the Eocene record occur between about 53.5 and 52.5 Ma (Figure 7b), reaching $\delta^{13}C$ values that approach even those seen at the PETM. Shortly thereafter, $\delta^{13}C$ values increase steadily to an early Eocene peak at 50 Ma. From the early/middle Eocene boundary $\delta^{13}C$ decreases until 46 Ma. The $\delta^{13}C$ data then remain relatively unchanged until 44 Ma. From 44 to 42 Ma a trend to higher $\delta^{13}C$ values and increased $\delta^{13}C$ variability is apparent. This corresponds with the time interval during

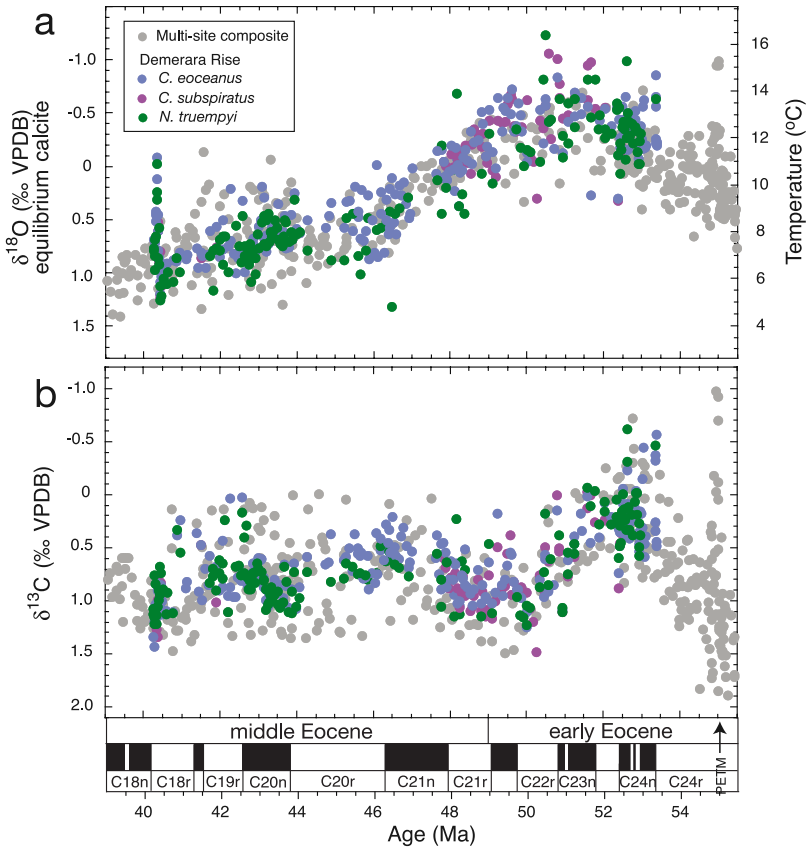


**Figure 7.** Multispecies benthic foraminiferal (a) $\delta^{18}O$ and (b) $\delta^{13}C$ data sets from Demerara Rise versus the composite data from Figure 6. Demerara Rise $\delta^{18}O$ data for *C. eoceanus* and *C. subspiratus* are corrected for disequilibrium fractionation with respect to seawater $\delta^{18}O$ using the "*Cibicidoides* spp.–*Oridorsalis*" offset of +0.28‰ [*Katz et al.*, 2003]. *N. truempyi* $\delta^{18}O$ data are corrected for disequilibrium fractionation using the offset for *Nuttallides* of +0.35‰ [*Shackleton et al.*, 1984; *Shackleton and Hall*, 1997]. The $\delta^{18}O$-temperature scale is computed for an "ice-free world" (global mean $\delta^{18}O_w = -1.27$‰ VPDB). Demerara Rise $\delta^{13}C$ data are normalized to *Cibicidoides* using the Demerara Rise interspecies $\delta^{13}C$ offset from Figure 5. Composite $\delta^{13}C$ data are as in Figure 6. Spread in Demerara Rise data for any given age reflects the presence of higher-frequency "Milankovitch" signals aliased by low-resolution sampling not noise. An interval of warmth in Southern Ocean records (ODP Site 689) occurs at about 41.5 Ma and is now documented as the apparent Middle Eocene Climatic Optimum (MECO) of *Bohaty and Zachos* [2003]. There is no corresponding warming registered at 41.5 Ma in the Demerara Rise records. However, recent refinements to age models at Sites 689 and 690 based on revised nannofossil biostratigraphy and magnetobiostratigraphic correlations [*Falkowski et al.*, 2005] suggest that the interval of Southern Ocean warmth represented by MECO actually occurred earlier at about 42.7 Ma. This earlier age is more consistent with the contemporaneous interval of relative warmth registered at Demerara Rise.

which $\delta^{18}O$ values register a temporary reversal in the middle Eocene long-term $\delta^{18}O$ increase. Finally, greater variability in $\delta^{13}C$ is coincident with the large-amplitude negative excursion in $\delta^{18}O$ at 40.35 Ma.

## 8. Early to Middle Eocene Upper Abyssal Ocean Temperatures

[23] Figure 7a shows warm upper abyssal temperatures in the western tropical Atlantic during the early Eocene. Peak temperatures from Demerara Rise (15° to 16°C) are the warmest yet reported for the deep oceans of the Eocene. More typically, temperatures fall in the region of 11° to 14°C, in broad agreement with the composite $\delta^{18}O$ data, recently reported $\delta^{18}O$ data from the Pacific [*Dutton et al.*, 2005] and benthic foraminiferal Mg/Ca [*Lear et al.*, 2000]. Elsewhere, it has been suggested that Paleogene and mid-Cretaceous deep ocean warmth of this magnitude can be explained by sinking of subtropical saline surface waters driven by excess evaporation in these latitudes [*Chamberlin*, 1906; *Brass et al.*, 1982; *Saltzman and Barron*, 1982; *Oberhansli and Hsu*, 1986; *Kennett and Stott*, 1990, 1991; *Pak and Miller*, 1992; *Zachos et al.*, 1993; *Thomas and Shackleton*, 1996; *Barrera et al.*, 1997]. Yet virtually no

data exist to support the notion of warm saline deep water (WSDW) formation in a subtropical region [*Crowley*, 1999]. The relatively high $\delta^{18}O$ values of molluscan calcite and early marine cements from mid-Cretaceous limestones from the Gulf of Mexico [*Woo et al.*, 1992] are often cited in support of the formation of subtropical WSDW. However, we now understand that the carbonates used may well have artificially high $\delta^{18}O$ values because of early marine diagenesis below the thermocline [*Wilson and Dickson*, 1996; *Poulsen et al.*, 1999].

[24] Deep water temperatures between 11 and 14°C during the early Eocene agree well with temperature reconstructions of Antarctic surface waters during this interval [*Stott et al.*, 1990], consistent with the idea that deep ocean warmth during the early Eocene greenhouse was attained by the subduction of warm high-latitude surface waters. This finding also agrees with numerical ocean general circulation modeling (OGCM) experiments which cast doubt on the physical plausibility of subduction of warm subtropical saline surface waters as an explanation for widespread early Eocene deep ocean warmth [*Bice and Marotzke*, 2001; *Huber and Sloan*, 2001]. After the acme of early Eocene warmth at 50.5 Ma, upper abyssal temperatures at Demerara Rise begin a steady decline, a trend that continues to 44 Ma. Between 44 and 42 Ma, a temporary reversal in the middle Eocene cooling trend is evident. During this interval temperatures rise from a background of 8°C to a maximum of 10°C. A pattern of deep ocean warming interrupting the middle Eocene cooling trend has also been documented in benthic foraminiferal stable isotope records from the Southern Ocean [*Barrera and Huber*, 1991; *Diester-Haass and Zahn*, 1996; *Bohaty and Zachos*, 2003]. Crucially, however, the interval of warmth in the Southern Ocean records occurs at about 41.5 Ma (the apparent "MECO" (Middle Eocene Climatic Optimum) of *Bohaty and Zachos* [2003]), whereas the interval of warmth documented at Demerara Rise is of a longer duration and occurs earlier, between 44 and 42 Ma (However, recent refinements to age models at Sites 689 and 690 based on revised nannofossil biostratigraphy and magnetobiostratigraphic correlations [*Falkowski et al.*, 2005] suggest that the interval of Southern Ocean warmth represented by "MECO" actually occurred earlier at about 42.7 Ma. This earlier age is more consistent with the contemporaneous interval of relative warmth registered at Demerara Rise). At about 42 Ma, cooling resumes at Demerara Rise until 40.35 Ma at which point a substantial short-lived transient warming is seen (6°C over ~60 kyr), a feature not detectable within the lower-resolution composite record [*Zachos et al.*, 2001] or seen in the Southern Ocean drill sites [*Bohaty and Zachos*, 2003].

## 9. Eocene Water Mass Ageing Gradients

[25] While the practice of comparing $\delta^{13}C$ data in benthic foraminiferal calcite from multiple sites and different ocean basins is one of the main sources of noise in a secular composite record of global change, it is also a means of obtaining valuable paleoceanographic information; interbasin $\delta^{13}C$ gradients provide a way to assess patterns of water mass ageing. Figure 8 shows Demerara Rise $\delta^{13}C$ data plotted together with the multisite composite $\delta^{13}C$ data [*Zachos et al.*, 2001] on an ocean-by-ocean basis. The $\delta^{18}O$ data sets for Demerara Rise and the "composite" sites are also shown in order to present the $\delta^{13}C$ interocean gradients in a climatic context. In order to remove intertaxa offsets in carbon isotope fractionation, both the composite and the Demerara Rise benthic foraminiferal $\delta^{13}C$ data have been normalized to "*Cibicidoides*." Demerara Rise $\delta^{13}C$ data are normalized using the offset (*C. eoceanus – N. truempyi* = +0.40‰) calculated at Demerara Rise shown in Figure 5. However, because the composite data are sourced from a variety of locations in all ocean basins and across a range of water depths, composite $\delta^{13}C$ data are normalized to *Cibicidoides* using the *Katz et al.* [2003] *Cibicidoides spp.–N. truempyi* offset of +0.34‰. The $\delta^{13}C$ data for Southern Ocean Sites 689 and 690 are plotted using the new age model for these sites [*Falkowski et al.*, 2005].

[26] Figure 8 emphasizes the substantially increased density of data coverage through the early and middle Eocene provided by our new Demerara Rise data. During the early Eocene (55 to 49 Ma) the $\delta^{13}C$ (and $\delta^{18}O$) data from different basins are remarkably similar, suggesting a rather homogenous global ocean with respect to the $\delta^{13}C$ of $\Sigma CO_2$ and temperature (interval "I," Figure 8). This observation can be explained by two different circulation regimes. One possibility is that multiple, spatially disparate sources of deep water existed during the early Eocene, with consequently less opportunity for prolonged deep water ageing to impart significant $\delta^{13}C$ differences between water masses. However, greater heterogeneity in deep ocean temperature might be expected under this scenario, in contrast to the relatively homogenous interbasin temperatures implied by the $\delta^{18}O$ records. A second possibility is a single dominant deep water source but with small ageing gradients, implying a less efficient biological pump than exists today.

[27] Toward the end of the early Eocene, interbasin $\delta^{13}C$ gradients begin to increase (interval "II," 48 to 50 Ma). As highlighted by the $\delta^{18}O$ data, this coincides with the termination of the sustained global warmth of the early Eocene and the initiation of middle Eocene global cooling. As global cooling progresses, interbasin $\delta^{13}C$ gradients intensify (interval "III"), primarily a result of decreasing $\delta^{13}C$ values in the Pacific, tropical Atlantic and Southern Ocean (although note the anomalous behavior of data from Site 527 during this interval). Composite data for this interval ("III") of the middle Eocene come from the Southern Ocean Atlantic sector Sites 690 and 689, with additional data from Site 527 in the southern South Atlantic (here grouped into "Southern Ocean, Atlantic"), high-latitude Indian Sites 738 and 757 ("Indian") and equatorial Pacific Site 865 ("Pacific"). Both the Pacific and the Indian Ocean ODP Sites 865, 738 and 757 lay at relatively shallow paleodepths (~1500 m) [*Weissel et al.*, 1989; *Barrera and Huber*, 1991; *Winterer et al.*, 1993], compared to Demerara Rise and Maud Rise ODP Site 690 (~2500–3000 m) [*Kennett et al.*, 1988; *Erbacher et al.*, 2004]. However, data from Sites 738, 757 and 865 span the period before, during and after the $\delta^{13}C$ divergence in interval "III", indicating that the divergence in $\delta^{13}C$ during interval "III" is not an artifact of the offset in depths among the sites but instead

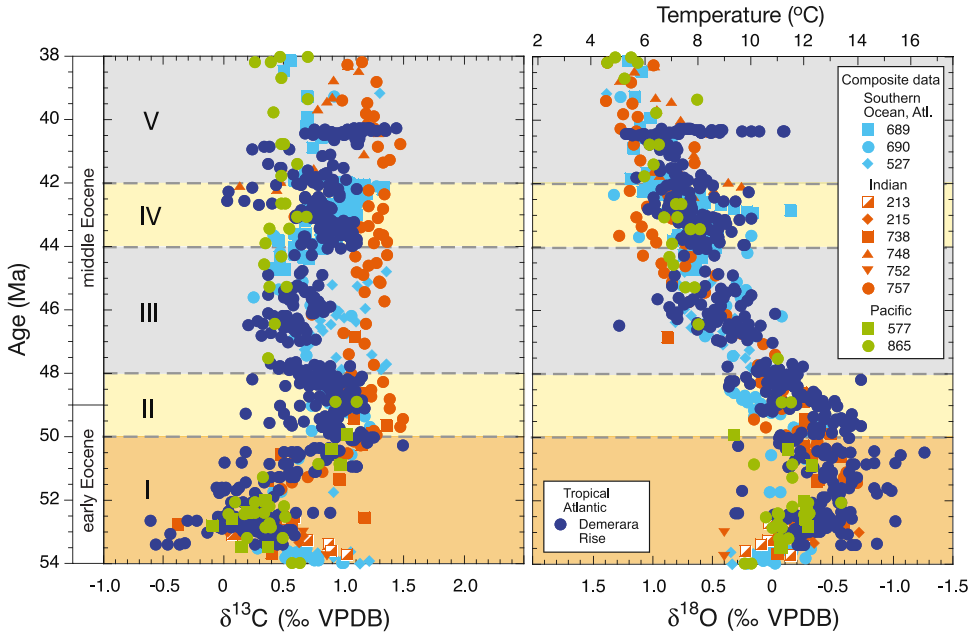


**Figure 8.** Multispecies benthic foraminiferal $\delta^{13}C$ data from Demerara Rise (data from Figure 7b) versus the composite multisite $\delta^{13}C$ data (from Figure 6b) with composite data from component sites plotted by ocean basin (see Figure 2a for site locations). For component drill sites within each basin, see legend. Demerara Rise $\delta^{13}C$ data are normalized to *Cibicidoides* using the Demerara Rise interspecies $\delta^{13}C$ offset from Figure 5. The $\delta^{13}C$ data from composite sites for *Nuttallides* are normalized to *Cibicidoides* using the *Cibicidoides* – *N. truempyi* $\delta^{13}C$ offset of +0.34 from *Katz et al.* [2003]. Intervals are denoted as follows: The $\delta^{13}C$ data from different basins are remarkably similar (interval I). The $\delta^{13}C$ data begin to display divergence (interval II). The $\delta^{13}C$ data from "Pacific," "Southern Ocean, Atlantic," and "tropical Atlantic" (Demerara Rise) sites diverge to lower $\delta^{13}C$ compared to "Indian" (interval III). The $\delta^{13}C$ interbasin divergence then weakens (interval IV) and becomes more similar to that evident in interval II. The $\delta^{13}C$ gradients strengthen again (interval V). These trends appear to display a covariance with the magnitude of deep ocean warmth through the Eocene. Colored horizontal bars qualitatively denote magnitude of deep ocean warmth: peach, very warm; yellow, warm; and grey, cooler. All data for composite sites are plotted using their age models from *Zachos et al.* [2001] apart from data from ODP Sites 689 and 690. These data are plotted using recent refinements to age models at these sites based on revised nannofossil biostratigraphy and magnetobiostratigraphic correlations [*Falkowski et al.*, 2005].

represents a change in interbasin gradients in seawater $\delta^{13}C$. These observations suggest that during interval "III" (44 to 48 Ma) the predominant location for deep water formation was close to the Indian sector of the Southern Ocean. During the temporary reversal in the middle Eocene cooling trend from 42 to 44 Ma, interbasin $\delta^{13}C$ gradients weaken (interval "IV"), a reversion to a situation similar to that witnessed during climatically warmer interval "II". With resumption of the middle Eocene global cooling trend at 42 Ma, $\delta^{13}C$ gradients increase again (interval "V").

[28] The correspondence between interbasin $\delta^{13}C$ gradients and deep ocean $\delta^{18}O$ values through the Eocene suggests that warmer climate regimes are associated with weaker water mass ageing gradients. Assuming that the spatial coverage of drill sites is representative of variability in Eocene deep ocean $\delta^{13}C$ of $\Sigma CO_2$, the association between water mass ageing gradients and background ocean temperatures can be explained in two ways. One possibility is that during the climatic warmth of the early Eocene the deep ocean was ventilated at multiple locations, whereas middle Eocene global cooling coincided with the appearance of a single dominant deep water source. Intervals "II" and "IV", across the early/middle Eocene boundary and from 42 to 44 Ma respectively, represent transitional intervals between these end-member regimes. Alternatively, the link between patterns of water mass ageing and background ocean temperatures could arise from a climatic influence on the efficiency with which the biological pump operates, with suppressed export production during climatically warm intervals causing weaker interbasin $\delta^{13}C$ gradients.

[29] The apparent link between climatic cooling and increased interbasin $\delta^{13}C$ gradients documented here for the Eocene may not necessarily hold for other epochs. For example, by at least earliest Oligocene time, interbasin $\delta^{13}C$ gradients had again become small or nonexistent [*Wright and Miller*, 1993], a situation similar to that of the early Eocene. The relatively low $\delta^{13}C$ signatures of the Atlantic and Pacific during the middle Eocene suggest the absence of

a northern component deep water source in either basin during this interval, corroborating evidence from early Eocene numerical ocean modeling experiments for deep water formation exclusively in the high southern latitudes [*Bice and Marotzke*, 2001]. From the combined evidence for patterns of interbasin $\delta^{13}C$ gradients, it appears that circulation patterns of the Eocene ocean were indeed significantly different from those of today.

## 10. Transient Climate Changes During the Eocene

[30] While the main purpose of this contribution is to address the reliability of multi-Myr timescale secular change seen in the published composite $\delta^{13}C$ and $\delta^{18}O$ records, the new records that we have presented show tantalizing preliminary evidence of the existence of a number of shorter-timescale "transient" events (timescale $\sim$ 100 kyr). Notably, we see indications of several potential "hyperthermal" events, akin to those hypothesized as having occurred periodically through the early Eocene interval of "greenhouse" warmth [*Thomas and Zachos*, 1999; *Thomas et al.*, 2000]. One of these events occurs at 52.6 Ma ("a" in Figure 9) while two others occur in close succession between 50.4 and 51.0 Ma ("b" and "c" in Figure 9). These events all exhibit negative excursions in both $\delta^{13}C$ and $\delta^{18}O$ of $\sim$1‰ and $\sim$0.8‰, respectively. The changes in $\delta^{18}O$ indicate rapid warmings of the upper abyssal tropical Atlantic by about 4°C. Support for the global nature of these events comes from recently generated bulk carbonate stable isotope records from the subtropical Pacific (DSDP Site 577) and midlatitude North Atlantic (DSDP Site 550) from the late Paleocene through early Eocene [*Cramer et al.*, 2003]. The $\delta^{13}C$ variability at the $\sim$100-kyr timescale was found to be paced by eccentricity-modulated precession cycles, with a particularly large-amplitude event occurring within C24n.1n (event "k" of *Cramer et al.* [2003]). This is coeval (to within the error of the $\sim$300-kyr duration of C24n.1n) to our event "a" in Figure 9.

[31] A fourth transient deep ocean warming, at 40.35 Ma during the late middle Eocene, is highlighted in Figure 10. This event is restricted to planktic foraminiferal biozone E12 (using the new Eocene planktic foraminifer zonation ("E" zones) of *Berggren and Pearson* [2005]; equals P13 using the "P" zones of *Berggren et al.* [1995]). E12 is one of the shortest biozones ($\sim$400-kyr duration) of the entire Cenozoic, defined by the total range of its distinctive "orbuline" marker species, *Orbulinoides beckmanni*. This event is distinct from those discussed above in that the negative excursion in $\delta^{18}O$ is not accompanied by a negative excursion in $\delta^{13}C$, suggesting that the mechanisms linking deep ocean temperature and carbon cycling were different during this event. If the 1.3‰ negative excursion in $\delta^{18}O$ is attributed wholly to temperature change, a warming of abyssal waters by about 6°C occurred within about 60 kyr. The 40.35 Ma event is also marked by a coeval decrease in the epifaunal (i.e., *C. eoceanus*) to shallow infaunal (i.e., *N. truempyi*) gradient in $\delta^{13}C$ ($\Delta\delta^{13}C$), suggesting a possible decline in export production coincident with the rapid deep ocean warming.

[32] It is also notable that the abrupt 1.3‰ decrease in $\delta^{18}O$ at 40.35 Ma occurs approximately coeval (within circa 400 kyr) with a 0.5‰ decrease in benthic foraminiferal $\delta^{18}O$ in the equatorial Pacific [*Tripati et al.*, 2005]. This 0.5‰ decrease followed a rapid shoaling of the calcite compensation depth (CCD) in the equatorial Pacific of $\sim$1 km [*Lyle et al.*, 2002], and has been interpreted as marking a deglaciation following a prior buildup of continental ice >100% of the modern Antarctic volume [*Tripati et al.*, 2005]. This line of argument follows the documented relationship between CCD deepening and the well-established large-scale Antarctic ice sheet expansion during the earliest Oligocene [*Coxall et al.*, 2005]. However, caution is warranted. Our new records from Demerara Rise do not indicate the positive excursions in $\delta^{18}O$ that would be expected to accompany the growth of a substantial continental ice sheet. In fact, the only significant excursions in $\delta^{18}O$ that are evident through the middle Eocene are excursions to more negative values.

## 11. Conclusions

[33] New early to middle Eocene benthic foraminiferal stable isotope data from Demerara Rise provide consistent, robust interspecies offsets which allow us to improve constraints on stable isotope offsets between species of *Cibicidoides* and *Nuttallides*, two commonly used benthic foraminiferal taxa in Eocene paleoceanographic studies. Despite several potential sources of noise inherent in multisite "composite" stable isotope stratigraphies, the validity of the composite $\delta^{18}O$ record for the early and middle Eocene, at least at multi-Myr timescales, has been confirmed by generating new monospecific records from a single location with good stratigraphic control. By removing sources of noise in the composite $\delta^{13}C$ record, our new $\delta^{13}C$ data provide a clearer signal of changes in carbon cycling through the early to middle Eocene.

[34] The pattern of Eocene paleoceanographic evolution as depicted in the Demerara Rise benthic foraminiferal $\delta^{18}O$ records provides clear support for a temporary reversal ($\sim$44 to 42 Ma) in the long-term climatic deterioration between the early Eocene and the late Eocene. This phase of warming punctuating the middle Eocene global cooling trend may correspond with a similar phase of warmth recorded in Southern Ocean drill sites (previously dated at 41.5 Ma) [*Bohaty and Zachos*, 2003] when using new age models for these sites [*Falkowski et al.*, 2005].

[35] Deconvolution of composite $\delta^{13}C$ data into component ocean basins, combined with the new $\delta^{13}C$ data set from Demerara Rise, allows us to assess secular change in interbasin $\delta^{13}C$ gradients and, by inference, patterns of water mass ageing. A strong correlation between interbasin $\delta^{13}C$ gradients and deep ocean $\delta^{18}O$ values suggests a link between patterns of water mass ageing and background ocean temperatures during the Eocene. Minimal interbasin $\delta^{13}C$ gradients during the warmest intervals of the Eocene (especially the early Eocene) may imply that multiple deep water sources are a feature of these warm climate regimes. Alternatively, minimal interbasin $\delta^{13}C$ gradients during warmer climates may have arisen from a reduction in the

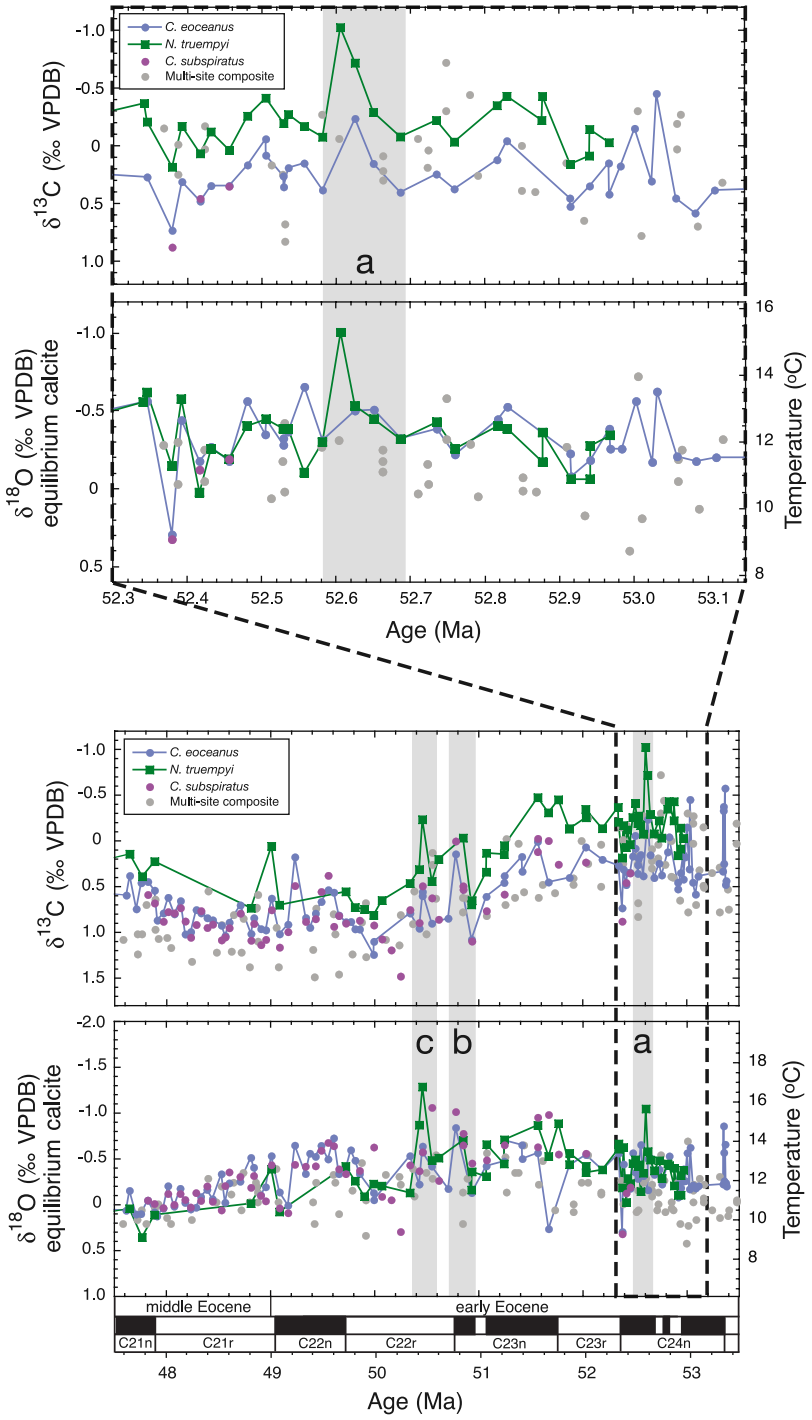


**Figure 9.** Demerara Rise benthic foraminiferal stable isotope data (from Figure 7) versus the composite data (from Figure 6) for the early middle through early Eocene interval from 47.5 to 53.5 Ma. Species symbol colors are the same as those in Figure 7. Shaded areas (labeled a, b, and c) denote intervals of large-amplitude negative excursions in both $\delta^{18}O$ and $\delta^{13}C$. All composite data are plotted using their original age model from *Zachos et al.* [2001].

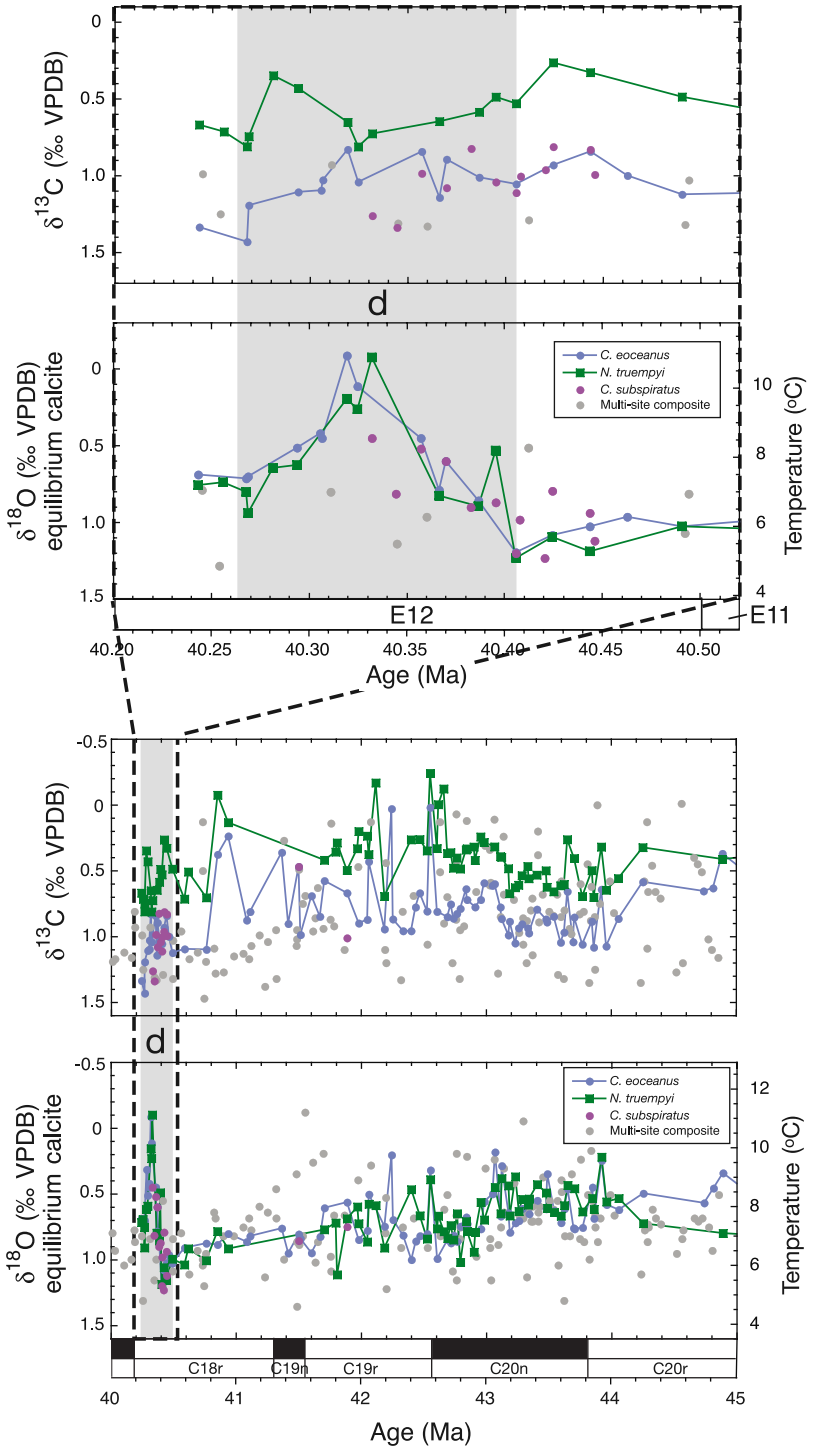


**Figure 10.** Demerara Rise benthic foraminiferal stable isotope data (from Figure 7) versus the composite data (from Figure 6), for the middle Eocene interval from 40 to 45 Ma. Species symbol colors are the same as those in Figure 7. Shaded area (d) denotes interval coinciding with a rapid (∼60 kyr) and large-amplitude (∼1.3‰) negative excursion in $\delta^{18}O$, corresponding with a decrease in the intertaxa (*C. eoceanus*–*N. truempyi*) offset in $\delta^{13}C$. All composite data are plotted using their original age model from *Zachos et al.* [2001].

efficiency of the biological pump causing weaker ageing gradients throughout the deep ocean. The relatively low $\delta^{13}C$ signatures of the Atlantic and Pacific oceans during the middle Eocene suggest the absence of a northern component deep water source in either basin during this interval.

[36] Demerara Rise $\delta^{13}C$ and $\delta^{18}O$ records show preliminary evidence for several intervals of short-lived transient climate instability in the early and middle Eocene where composite data are particularly sparse, most notably at 52.6 (C24n.1n), 50.5 (C22r) and 40.3 (C18r) Ma. The last of these events is composed of a pronounced (~1.3‰) and rapid (~60 kyr) negative $\delta^{18}O$ excursion punctuating the middle Eocene trend toward increasingly positive $\delta^{18}O$. Interpreted solely in terms of temperature change, this negative $\delta^{18}O$ excursion signifies a sudden warming of the deep ocean by at least 6°C.

[37] **Acknowledgments.** We thank the Shipboard Party of Ocean Drilling Program Leg 207 for a successful drilling expedition and Mike Bolshaw, Matt Cooper, and Paula Worstell for laboratory assistance. We also thank Dick Kroon, John Murray, and Heiko Pälike for useful discussions and comments on an earlier draft of the manuscript. Reviews from an anonymous reviewer and from Miriam Katz, in particular, were very thorough and extremely helpful. Helen Coxall provided SEM images of benthic foraminifera from DSDP Site 522. This research used samples provided by the Ocean Drilling Program. Financial support for this research was provided by Natural Environment Research Council studentship GT04/00/ES/250 (to P.F.S.), NERC UK ODP grant NE/B50004X/1 (to P.A.W.), USSSP postcruise funding (to R.D.N.), and an NSF-OCE grant (to R.D.N.).

## References


Arthur, M. A., and J. H. Natland (1979), Carbonaceous sediments in the North and South Atlantic: The role of salinity in stable stratification of Early Cretaceous basins, in *Deep Drilling Results in the Atlantic Ocean: Continental Margins and Paleoenvironment*, *Maurice Ewing Ser.*, vol. 3, edited by M. Talwani et al., pp. 375–401, AGU, Washington, D. C.

Aubry, M.-P. (1995), From chronology to stratigraphy: Interpreting the lower and middle Eocene stratigraphic record in the Atlantic Ocean, in *Geochronology, Time Scales and Global Stratigraphic Correlation*, edited by W. A. Berggren et al., *Spec. Publ. SEPM Soc. Sediment. Geol.*, *54*, 213–274.

Barrera, E., and B. T. Huber (1991), Paleogene and early Neogene oceanography of the southern Indian Ocean: Leg 119 foraminifer stable isotope results, *Proc. Ocean Drill. Program Sci. Results*, *119*, 693–717.

Barrera, E., S. M. Savin, E. Thomas, and C. E. Jones (1997), Evidence for thermohaline-circulation reversals controlled by sea-level change in the latest Cretaceous, *Geology*, *25*, 715–718.

Barron, E. J., P. J. Fawcett, W. H. Peterson, D. Pollard, and S. L. Thompson (1995), A "simulation" of mid-Cretaceous climate, *Paleoceanography*, *10*, 953–962.

Belanger, P. E., W. B. Curry, and R. K. Matthews (1981), Core-top evaluation of benthic foraminiferal isotopic-ratios for paleo-oceanographic interpretations, *Palaeogeogr. Palaeoclimatol. Palaeoecol.*, *33*, 205–220.

Bemis, B. E., H. J. Spero, J. Bijma, and D. W. Lea (1998), Reevaluation of the oxygen isotopic composition of planktonic foraminifera: Experimental results and revised paleotemperature equations, *Paleoceanography*, *13*, 150–160.

Berggren, W. A., and P. N. Pearson (2005), A revised tropical to subtropical Paleogene planktonic foraminiferal zonation, *J. Foraminiferal Res.*, *35*, 279–298.

Berggren, W., D. Kent, and C. Swisher III (1995), A revised Cenozoic geochronology and chronostratigraphy, in *Geochronology Time Scales and Global Stratigraphic Correlation*, edited by W. Berggren et al., *Spec. Publ. SEPM Soc. Sediment. Geol.*, *54*, 129–212.

Berner, R. A., and Z. Kothavala (2001), GEOCARB III: A revised model of atmospheric $CO_2$ over phanerozoic time, *Am. J. Sci.*, *301*, 182–204.

Berner, R. A., A. C. Lasaga, and R. M. Garrels (1983), The carbonate-silicate geochemical cycle and its effect on atmospheric carbon-dioxide over the past 100 million years, *Am. J. Sci.*, *283*, 641–683.

Bice, K. L., and J. Marotzke (2001), Numerical evidence against reversed thermohaline circulation in the warm Paleocene/Eocene ocean, *J. Geophys. Res.*, *106*, 11,529–11,542.

Bice, K. L., and R. D. Norris (2002), Possible atmospheric $CO_2$ extremes of the Middle Cretaceous (late Albian-Turonian), *Paleoceanography*, *17*(4), 1070, doi:10.1029/2002PA000778.

Bohaty, S. M., and J. C. Zachos (2003), Significant Southern Ocean warming event in the late middle Eocene, *Geology*, *31*, 1017–1020.

Bralower, T. J., J. C. Zachos, E. Thomas, M. Parrow, C. K. Paull, D. C. Kelly, I. P. Silva, W. V. Sliter, and K. C. Lohmann (1995), Late Paleocene to Eocene paleoceanography of the equatorial Pacific Ocean: Stable isotopes recorded at Ocean Drilling Program Site 865, Allison Guyot, *Paleoceanography*, *10*, 841–865.

Brass, G. W., J. R. Southam, and W. H. Peterson (1982), Warm saline bottom water in the ancient ocean, *Nature*, *296*, 620–623.

Cande, S. C., and D. V. Kent (1995), Revised calibration of the geomagnetic polarity timescale for the Late Cretaceous and Cenozoic, *J. Geophys. Res.*, *100*, 6093–6095.

Chamberlin, T. C. (1906), On a possible reversal of deep sea circulation and its influence on geologic climates, *J. Geol.*, *14*, 363–373.

Coxall, H. K., P. A. Wilson, H. Pälike, C. H. Lear, and J. Backman (2005), Rapid stepwise onset of Antarctic glaciation and deeper calcite compensation in the Pacific Ocean, *Nature*, *433*, 53–57.

Cramer, B. S., J. D. Wright, D. V. Kent, and M.-P. Aubry (2003), Orbital climate forcing of $\delta^{13}C$excursions in the late Paleocene–early Eocene (chrons C24n–C25n), *Paleoceanography*, *18*(4), 1097, doi:10.1029/2003PA000909.

Crowley, T. J. (1999), Paleomyths I have known, in *Modeling the Earth's Climate and Its Variability*, edited by W. R. Holland, S. Joussame, and F. David, pp. 377–430, Elsevier, New York.

Curry, W. B., J. C. Duplessy, L. D. Labeyrie, and N. J. Shackleton (1988), Changes in the distribution of $^{13}C$ of deep water $CO_2$ between the last glaciation and the Holocene, *Paleoceanography*, *3*, 317–341.

Curry, W. B., N. C. Slowey, and G. P. Lohmann (1993), Oxygen and carbon isotopic fractionation of aragonitic and calcitic benthic foraminifera on Little Bahama Bank, Bahamas (abstract), *Eos Trans. AGU*, *74*(43), Fall Meet. Suppl., 368.

de Menocal, P. B., D. W. Oppo, R. G. Fairbanks, and W. Prell (1992), Pleistocene $\delta^{13}C$ variability of North Atlantic intermediate water, *Paleoceanography*, *7*, 229–250.

Diester-Haass, L., and R. Zahn (1996), Eocene-Oligocene transition in the Southern Ocean: History of water mass circulation and biological productivity, *Geology*, *24*, 163–166.

Duplessy, J. C., N. J. Shackleton, R. K. Matthews, W. Prell, W. F. Ruddiman, M. Caralp, and C. H. Hendy (1984), C-13 record of benthic foraminifera in the last interglacial Ocean—Implications for the carbon-cycle and the global deep-water circulation, *Quat. Res.*, *21*, 225–243.

Dutton, A., K. C. Lohmann, and R. M. Leckie (2005), Insights from the Paleogene tropical Pacific: Foraminiferal stable isotope and elemental results from Site 1209, Shatsky Rise, *Paleoceanography*, *20*, PA3004, doi:10.1029/2004PA001098.

Ekart, D. D., T. E. Cerling, I. P. Montanez, and N. J. Tabor (1999), A 400 million year carbon isotope record of pedogenic carbonate: Implications for paleoatmospheric carbon dioxide, *Am. J. Science*, *299*, 805–827.

Erbacher, J., et al. (2004), *Demerara Rise: Equatorial Cretaceous and Paleogene Equatorial Paleoceanographic Transect, Western Atlantic* [online], vol. 207, Ocean Drill. Program, College Station, Tex. (Available at http://www-odp.tamu.edu/publications/207_IR/207TOC.HTM)

Falkowski, P. G., M. E. Katz, A. J. Milligan, K. Fennel, B. S. Cramer, M. P. Aubry, R. A. Berner, M. J. Novacek, and W. M. Zapol (2005), The rise of oxygen over the past 205 million years and the evolution of large placental mammals, *Science*, *309*, 2202–2204.

Graham, D. W., B. H. Corliss, M. L. Bender, and L. D. Keigwin (1981), Carbon and oxygen isotopic disequilibria of recent deep-sea benthic foraminifera, *Mar. Micropaleontol.*, *6*, 483–497.

Greenwood, D. R., and S. L. Wing (1995), Eocene continental climates and latitudinal temperature gradients, *Geology*, *23*, 1044–1048.

Huber, M., and L. C. Sloan (2001), Heat transport, deep waters, and thermal gradients:

Coupled simulation of an Eocene greenhouse climate, *Geophys. Res. Lett.*, *28*, 3481–3484.
Jorissen, F. J., and I. Wittling (1999), Ecological evidence from live-dead comparisons of benthic foraminiferal faunas off Cape Blanc (northwest Africa), *Palaeogeogr. Palaeoclimatol. Palaeoecol.*, *149*, 151–170.
Jorissen, F. J., I. Wittling, J. P. Peypouquet, C. Rabouille, and J. C. Relexans (1998), Live benthic foraminiferal faunas off Cape Blanc, NW-Africa: Community structure and microhabitats, *Deep Sea Res., Part I*, *45*, 2157–2188.
Kaiho, K. (1998), Phylogeny of deep-sea calcareous trochospiral benthic foraminifera: Evolution and diversification, *Micropaleontology*, *44*, 291–311.
Katz, M. E., D. R. Katz, J. D. Wright, K. G. Miller, D. K. Pak, N. J. Shackleton, and E. Thomas (2003), Early Cenozoic benthic foraminiferal isotopes: Species reliability and interspecies correction factors, *Paleoceanography*, *18*(2), 1024, doi:10.1029/2002PA000798.
Kennett, J., and L. Stott (1990), Proteus and Proto-Oceanus: Ancestral Paleogene oceans as revealed from Antarctic stable isotopic results, ODP Leg 113, *Proc. Ocean Drill. Program Sci. Results*, *113*, 865–880.
Kennett, J. P., and L. D. Stott (1991), Abrupt deep-sea warming, palaeoceanographic changes and benthic extinctions at the end of the Paleocene, *Nature*, *353*, 225–229.
Kennett, J. P., et al. (Eds.) (1988), *Initial Reports Ocean Drilling Program, Leg 113*, Ocean Drill. Program, College Station, Tex.
Kim, S. T., and J. R. O'Neil (1997), Equilibrium and nonequilibrium oxygen isotope effects in synthetic carbonates, *Geochim. Cosmochim. Acta*, *61*, 3461–3475.
Larson, R. L. (1991), Geological consequences of superplumes, *Geology*, *19*, 963–966.
Lear, C. H., H. Elderfield, and P. A. Wilson (2000), Cenozoic deep-sea temperatures and global ice volumes from Mg/Ca in benthic foraminiferal calcite, *Science*, *287*, 269–272.
Lear, C. H., Y. Rosenthal, and N. Slowey (2002), Benthic foraminiferal Mg/Ca-paleothermometry: A revised core-top calibration, *Geochim. Cosmochim. Acta*, *66*, 3375–3387.
Lyle, M. W., et al. (2002), *Leg 199 Preliminary Report* [online], *Ocean Drill. Program Prelim. Rep.*, vol. 99. (Available at http://www-odp.tamu.edu/publications/prelim/199_prel/199PREL.PDF)
Miller, K. G., J. D. Wright, and R. G. Fairbanks (1991), Unlocking the ice house—Oligocene-Miocene oxygen isotopes, eustasy, and margin erosion, *J. Geophys. Res.*, *96*, 6829–6848.
Mix, A. C., N. G. Pisias, R. Zahn, W. Rugh, J. Wilson, A. Morey, and T. K. Hagelberg (1995), Benthic foraminifer stable isotope record from site 849 (0–5 Ma): Local and global climate changes, *Proc. Ocean Drill. Program Sci. Results*, *138*, 371–412.
Norris, R. D., A. Klaus, and D. Kroon (2001), Mid-Eocene deep water, the late Palaeocene thermal maximum and continental slope mass wasting during the Cretaceous-Palaeogene impact, in *Western North Atlantic Palaeogene and Cretaceous Paleoceanography*, edited by D. Kroon, R. D. Norris, and A. Klaus, pp. 23–48, Geol. Soc. of London, London.
Oberhansli, H., and K. J. Hsu (1986), Palaeocene-Eocene palaeoceanography, in *Mesozoic and Cenozoic Oceans*, edited by K. J. Hsu, pp. 85–100, AGU, Washington D. C.
Pagani, M., J. C. Zachos, K. H. Freeman, B. Tipple, and S. Bohaty (2005), Marked decline in atmospheric carbon dioxide concentrations during the Paleogene, *Science*, *309*, 600–603.
Pak, D. K., and K. G. Miller (1992), Paleocene to Eocene benthic foraminiferal isotopes and assemblages: Implications for deepwater circulation, *Paleoceanography*, *7*, 405–422.
Pearson, P. N., and M. R. Palmer (2000), Atmospheric carbon dioxide concentrations over the past 60 million years, *Nature*, *406*, 695–699.
Poulsen, C. J., E. J. Barren, W. H. Peterson, and P. A. Wilson (1999), A reinterpretation of mid-Cretaceous shallow marine temperatures through model-data comparison, *Paleoceanography*, *14*, 679–697.
Rice, D. L., and D. C. Rhoads (1989), Early diagenesis of organic matter and the nutritional value of sediment, in *Ecology of Marine Deposit Feeders*, edited by J. Lopez, G. Taghon, and J. Levinton, pp. 309–317, Springer, New York.
Saltzman, E. S., and E. J. Barron (1982), Deep circulation in the Late Cretaceous—Oxygen isotope paleotemperatures from Inoceramus remains in DSDP cores, *Palaeogeogr. Palaeoclimatol. Palaeoecol.*, *40*, 167–181.
Sarnthein, M., K. Winn, J.-C. Duplessy, and M. R. Fontugne (1988), Global variations of surface ocean productivity in low and mid latitudes: Influence on $CO_2$ reservoirs of the deep ocean and atmosphere during the last 21,000 years, *Paleoceanography*, *3*, 361–399.
Shackleton, N. J., and M. A. Hall (1997), The late Miocene stable isotope record, Site 926, *Proc. Ocean Drill. Program Sci. Results*, *154*, 367–373.
Shackleton, N. J., M. A. Hall, and A. Boersma (1984), Oxygen and carbon isotope data from Leg-74 foraminifers, *Initial Rep. Deep Sea Drill. Project*, *74*, 599–612.
Shellito, C. J., L. C. Sloan, and M. Huber (2003), Climate model sensitivity to atmospheric $CO_2$ levels in the early-middle Paleogene, *Palaeogeogr. Palaeoclimatol. Palaeoecol.*, *193*, 113–123.
Sloan, L. C., and D. K. Rea (1996), Atmospheric carbon dioxide and early Eocene climate: A general circulation modeling sensitivity study, *Palaeogeogr. Palaeoclimatol. Palaeoecol.*, *119*, 275–292.
Spero, H. J., J. Bijma, D. W. Lea, and B. E. Bemis (1997), Effect of seawater carbonate concentration on foraminiferal carbon and oxygen isotopes, *Nature*, *390*, 497–500.
Stott, L. D., J. P. Kennett, N. J. Shackleton, and R. M. Corfield (1990), The evolution of Antarctic surface water during the Palaeogene: Inferences from the stable isotopic composition of planktonic foraminifera, ODP Leg 113, *Proc. Ocean Drill. Program Sci. Results*, *113*, 849–863.
Suganuma, Y., and J. G. Ogg (2006), Campanian through Eocene magnetostratigraphy of Sites 1257–1261, ODP Leg 207, Demerara Rise (western equatorial Atlantic) [online], *Proc. Ocean Drill. Program, Sci. Results*, *207*, (Available at http://www-odp.tamu.edu/publications/207_SR/102/102.htm)
Thomas, E., and N. J. Shackleton (1996), The Palaeocene-Eocene benthic foraminiferal extinction and stable isotope anomalies, in *Correlation of the Early Paleogene in Northwest Europe*, edited by R. W. O. B. Knox, R. M. Corfield, and R. E. Dunay, pp. 401–441, Geol. Soc., London.
Thomas, E., and J. C. Zachos (1999), Isotopic, paleontologic, and other evidence for multiple transient thermal maxima in the Paleocene and Eocene, *Eos Trans. AGU*, *80*(46), Fall Meet. Suppl., F487.
Thomas, E., J. C. Zachos, and T. J. Bralower (2000), Deep sea environments on a warm Earth, in *Warm Climates in Earth History*, edited by B. Huber, K. MacLeod, and S. Wing, pp. 132–160, Cambridge Univ. Press, New York.
Tjalsma, R. C., and G. P. Lohmann (1983), Paleocene-Eocene bathyal and abyssal benthic foraminifera from the Atlantic Ocean, *Micropaleontology Spec. Publ.*, *4*, 90 pp.
Tripati, A., J. Backman, H. Elderfield, and P. Ferretti (2005), Eocene bipolar glaciation associated with global carbon cycle changes, *Nature*, *436*, 341–346.
van Morkhoven, F. P. C. M., W. A. Berggren, and A. S. Edwards (1986), *Cenozoic Cosmopolitan Deep Water Benthic Foraminifera*, 421 pp., Elf-Aquitaine, Pau, France.
Weissel, J. K., et al. (Eds.) (1989), *Initial Report of the Ocean Drilling Program, Leg 121*, Ocean Drill. Program, College Station, Tex.
Wilson, P. A., and J. A. D. Dickson (1996), Radiaxial calcite: Alteration product of and petrographic proxy for magnesian calcite marine cement, *Geology*, *24*, 945–948.
Wilson, P. A., and R. D. Norris (2001), Warm tropical ocean surface and global anoxia during the mid-Cretaceous period, *Nature*, *412*, 425–429.
Wilson, P. A., R. D. Norris, and M. J. Cooper (2002), Testing the Cretaceous greenhouse hypothesis using glassy foraminiferal calcite from the core of the Turonian tropics on Demerara Rise, *Geology*, *30*, 607–610.
Winterer, E., et al. (Eds.) (1993), *Init. Report of the Ocean Drilling Program, Leg 143*, Ocean Drill. Program, College Station, Tex.
Woo, K. S., T. F. Anderson, L. B. Railsback, and P. A. Sandberg (1992), Evidence for high salinity of surface seawater in the mid-Cretaceous Gulf of Mexico, *Paleoceanography*, *7*, 673–685.
Wright, J. D., and K. G. Miller (1993), Southern Ocean influence on late Eocene to Miocene deepwater circulation, in *The Antarctic Paleoenvironment: A Perspective on Global Change*, *Antarct. Res. Ser.*, vol. 60, edited by J. P. Kennett and D. A. Warnke, pp. 1–25, AGU, Washington, D. C.
Zachos, J. C., D. K. Rea, K. Seto, R. Nomura, and N. Niitsuma (1992), Paleogene and early Neogene deep water paleoceanography of the Indian Ocean as determined from benthic foraminifer stable carbon and oxygen isotope records, in *Synthesis of Results From Scientific Drilling in the Indian Ocean*, *Geophys. Monogr. Ser.*, vol. 70, edited by R. A. Duncan et al., pp. 351–386, AGU, Washington, D. C.
Zachos, J. C., K. C. Lohmann, J. C. G. Walker, and S. W. Wise (1993), Abrupt climate change and transient climates during the Paleogene—A marine perspective, *J. Geol.*, *101*, 191–213.
Zachos, J. C., L. D. Stott, and K. C. Lohmann (1994), Evolution of early Cenozoic marine temperatures, *Paleoceanography*, *9*, 353–387.
Zachos, J., M. Pagani, L. Sloan, E. Thomas, and K. Billups (2001), Trends, rhythms, and aberrations in global climate 65 Ma to present, *Science*, *292*, 686–693.

R. D. Norris, Geosciences Research Division, Scripps Institution of Oceanography, MS-0244, 308 Vaughan Hall, La Jolla, CA 92093-0244, USA.

P. F. Sexton and P. A. Wilson, National Oceanography Centre, Southampton, School of Ocean and Earth Science, European Way, Southampton SO14 3ZH, UK. (p.sexton@noc.soton.ac.uk)